CellPress
PARTNER JOURNAL

Molecular Plant
Resource Article

Machine Learning Techniques for Predicting Crop Photosynthetic Capacity from Leaf Reflectance Spectra

David Heckmann[1,4,*], Urte Schlüter[2,4] and Andreas P.M. Weber[2,3]

[1]Heinrich-Heine-Universität, Institute for Computer Science

[2]Heinrich-Heine-Universität, Institute of Plant Biochemistry

[3]Cluster of Excellence on Plant Sciences (CEPLAS) "From Complex Traits towards Synthetic Modules" 40225 Düsseldorf, Germany

[4]These authors contributed equally to this article.

***Correspondence: David Heckmann (david.heckmann@uni-duesseldorf.de)**

http://dx.doi.org/10.1016/j.molp.2017.04.009

ABSTRACT

Harnessing natural variation in photosynthetic capacity is a promising route toward yield increases, but physiological phenotyping is still too laborious for large-scale genetic screens. Here, we evaluate the potential of leaf reflectance spectroscopy to predict parameters of photosynthetic capacity in *Brassica oleracea* and *Zea mays*, a C_3 and a C_4 crop, respectively. To this end, we systematically evaluated properties of reflectance spectra and found that they are surprisingly similar over a wide range of species. We assessed the performance of a wide range of machine learning methods and selected recursive feature elimination on untransformed spectra followed by partial least squares regression as the preferred algorithm that yielded the highest predictive power. Learning curves of this algorithm suggest optimal species-specific sample sizes. Using the *Brassica* relative *Moricandia*, we evaluated the model transferability between species and found that cross-species performance cannot be predicted from phylogenetic proximity. The final intra-species models predict crop photosynthetic capacity with high accuracy. Based on the estimated model accuracy, we simulated the use of the models in selective breeding experiments, and showed that high-throughput photosynthetic phenotyping using our method has the potential to greatly improve breeding success. Our results indicate that leaf reflectance phenotyping is an efficient method for improving crop photosynthetic capacity.

Key words: leaf spectrometry, photosynthesis, machine learning, crops, C_4, phenotyping

Heckmann D., Schlüter U., and Weber A.P.M. (2017). Machine Learning Techniques for Predicting Crop Photosynthetic Capacity from Leaf Reflectance Spectra. Mol. Plant. **10**, 878–890.

INTRODUCTION

In the upcoming decades, the amount of arable land that is available per capita will continue to decrease. Thus, agriculture faces an enormous demand for the enhancement of sustainable crop production (Maurino and Weber, 2013). Improvements in plant photosynthetic efficiency are expected to play a major role in the efforts to increase agricultural productivity (Zhu et al., 2010; Long et al., 2015; Ort et al., 2015). Photosynthetic efficiency is not just connected to potential yield increases but also influences efficiency of the use of resources such as water and nitrogen. An important reason for the insufficient exploration of the potential for changes to photosynthesis for crop improvement is the lack of appropriate high-throughput screening methods, in particular with respect to parameters such as the maximal rate of carboxylation (V_{cmax}) and the maximal rate of electron transport (J_{max}). Knowledge of variation in these parameters can play an important role in preparing crops for the predicted global changes in CO_2 and temperature (Kromdijk and Long, 2016).

As the central part of plant metabolism, photosynthesis has to be in tune with all other vital processes. Under natural conditions, plants are usually not optimized for maximal biomass production or the maximal production of the harvest product, e.g., the grain. During the green revolution, major crop improvements could be achieved by changes in a few genes or even just a single gene. In rice, the introduction of the semidwarf gene *sd-1* interrupts

Published by the Molecular Plant Shanghai Editorial Office in association with Cell Press, an imprint of Elsevier Inc., on behalf of CSPB and IPPE, SIBS, CAS.

gibberellic acid production in the stem, leading to an increased resistance to lodging, a shift in biomass partitioning from the stem toward the grain (corresponding to an increase in harvest index), and consequently remarkable yield increases (Spielmeyer et al., 2002). In contrast, improvements in photosynthesis are thought to depend on much more complex genomic changes (Long et al., 2006). However, a number of recent developments raise the expectation that increases of photosynthetic capacity will significantly contribute to future crop improvements. These developments include an improved understanding of photosynthetic processes, the emergence of high-performance computing, and advances in genetic engineering (Long et al., 2015).

Continuous improvements in sequencing technologies have led to the development of genetically well-characterized breeding line collections, such as the multi-parent advanced generation inter-cross populations (MAGIC) in rice (Bandillo et al., 2013), wheat (Mackay et al., 2014), and corn (Dell'Acqua et al., 2015). However, the development of high-throughput phenotyping methods for the physiological characterization of these lines is lacking far behind, and the scarcity of phenotypic data currently presents a major bottleneck in plant improvement (Furbank and Tester, 2011; Fiorani and Schurr, 2013).

Automated phenotyping platforms have been set up in several research institutes, but their operation expenses are still high, and the number of individuals that can be tested is still relatively small. In addition, existing platforms provide only limited information on the photosynthetic performance of the screened material. So far, large-scale screens of photosynthesis mainly use pulse-amplitude modulated chlorophyll fluorescence (PAM) measurements (Harbinson et al., 2012; Harbinson, 2013). This technique relies on the relationship between CO_2 assimilation and associated changes in chlorophyll fluorescence in the illuminated leaf (Baker, 2008; Murchie and Lawson, 2013), which allows fast determination of the apparent PSII efficiency and electron transport rate. Unfortunately, this strategy makes fluorescence measurements very dependent on the current physiological status of the plant as well as on environmental conditions, especially light, during the measurements. PAM thus provides a snapshot of the current status of the photosynthetic apparatus; more general photosynthetic parameters such as the carboxylation activity or the maximal photosynthetic capacity require long-term experiments by gas exchange that are usually conducted with an infrared gas analyzer (IRGA). In C_3 plants, determination of an assimilation response curve to changes in internal CO_2 allows the estimation of V_{cmax}, the maximal carboxylation rate of Rubisco, which is closely related to the initial slope of the A-C_i curve, as well as J_{max}, the regeneration of ribulose 1,5-bisphosphate, which is closely related to the maximal assimilation rate at saturating CO_2. In C_4 plants, the A-C_i curve at very low CO_2 concentrations describes the PEP carboxylation rate, while at high CO_2 concentrations, it is governed by the electron transport rate supporting PEP regeneration (Long and Bernacchi, 2003; von Caemmerer, 2000). In contrast to fluorescence analysis, gas exchange measurements are very laborious and time consuming, and are therefore not suitable for high-throughput screenings.

A new method for fast and non-destructive assessment of the general photosynthetic capacity of plants was recently presented with the use of leaf spectral reflectance (Serbin et al., 2012; Ainsworth et al., 2014; Yendrek et al., 2017). The reflectance spectrum ranging from the visible over the near infrared to the intermediate infrared (ca. 350 to 2500 nm) gives information on the physical and chemical state as well as surface and texture properties of the material under investigation. It is widely used in geology as well as agriculture. Reflectance spectra from crop canopies facilitate the assessment of the plants' composition, nutritional status, as well as certain stress parameters. This includes estimates of nutrient composition (Gillon et al., 1999; Zhai et al., 2013), water content and water use efficiency (Wang et al., 2012a), chlorophyll content (Atzberger et al., 2010), cell wall composition (Penning et al., 2009), content of secondary metabolites (Couture et al., 2013; Jia et al., 2013), heavy metal content (Liu et al., 2010a), disease expansion (Xu et al., 2006; Mahlein et al., 2012), and species composition (Borregaard et al., 2000; Manevski et al., 2011). Reflectance-based evaluation of the nitrogen status of crop plants has been particularly successful; data for specific wavelengths (Alchanatis et al., 2005) or indices can be correlated to the nitrogen status of the plants (Zhao et al., 2005; Wang et al., 2012b; Bao et al., 2013; Ecarnot et al., 2013) over a wide range of species.

The use of linear regression or neural networks resulted in improved models for parameter prediction from spectral reflectance (Liu et al., 2010b; Kira et al., 2016), and these methodological improvements have also broadened the spectrum of parameters that can be estimated from such datasets. Additional innovation came from improved spectrometers with accessories such as the leaf clip containing a fixed internal light source, which reduces interference from the atmosphere, light quality, and light angle. In addition to the previously known relationships between leaf spectral reflectance and nitrogen or chlorophyll content, these advances allow the assessment of specific photosynthetic parameters in a variety of experimental setups. A relationship between leaf reflectance indices and photosynthetic parameters was shown for the first time in leaves of different forest trees (Doughty et al., 2011; Dillen et al., 2012). Serbin et al. (2012) were able to estimate the influence of temperature on photosynthesis parameters, such as V_{cmax} and J_{max}, in two different poplar species. Leaf reflectance data from ozone-treated soybean leaves or maize was also modeled for monitoring photosynthesis parameters (Ainsworth et al., 2014; Yendrek et al., 2017). These results raise hope that leaf spectral reflectance may also be suitable for photosynthetic phenotyping of crop plants.

Here, we describe pre-conditions for the setup of such a photosynthesis screening experiment. In particular, we address the following questions: (1) what is the natural variation in the leaf reflectance spectra of different plant groups?, (2) which computational methods are most suitable for building reliable models to predict photosynthetic capacity from reflectance spectra?, (3) what are the minimal experimental requirements for the development of a spectral reflectance model for photosynthetic parameters?, (4) can such models be transferred between species?, and (5) is the error of prediction low enough to allow selective breeding for photosynthetic capacity? The answers to these questions will help to facilitate the development of

high-throughput screening protocols and photosynthesis prediction models.

Our first experiment compares the reflectance spectra from mature leaves of representatives of 36 plant genera. Variation in this dataset is supposed to depend mainly on structural variation. Detailed modeling of the relationship between leaf reflectance spectra and photosynthesis parameters derived from A-C_i curves of gas exchange measurements are then performed based on data from our second experiment with the C_3 plant cabbage (*Brassica oleraceae*) and the C_4 plant corn (*Zea mays*). For several representatives of each species, we estimate leaf photosynthetic capacity through the initial slope and the maximum rate of the A-C_i curves (A_{max}, see Methods). In order to control and compare our system, models are also developed for the more established relationship between reflectance spectra and carbon-to-nitrogen (CN) ratio of the material. To assess the species specificity and the potential for cross-species transfer of the derived models, close phylogenetic relatives of *Brassica* with similar leaf structure in the genus *Moricandia* are also examined. In contrast to PSII fluorescence or gas exchange, reflectance spectroscopy represents estimates of photosynthetic parameters obtained by correlation. While our understanding of the underlying principles is still limited, the simplicity and speed of measurements will make it an efficient tool for the determination of photosynthetic variation in natural as well as breeding populations. Uncovering of photosynthesis variation in characterized plant material will help to explore its genetic basis and its potential for improving yield.

RESULTS

Spectra Lie in a Low-Dimensional Space over a Wide Range of Species

In order to understand the diversity and general properties of leaf clip reflectance spectra, we sampled reflectance spectra of 36 diverse species. This set of spectra was of surprisingly low diversity, with 97% of the variance contained in the first three principal components (Figure 1A). The spectra across a wide range of species thus lie in a low-dimensional space. The reason for this becomes apparent in the correlation matrix of the spectra (Figure 1B). Four major independent ranges of wavelengths are identified, within which measurements are strongly correlated. Two correlated ranges are found in the visible spectrum (from about 450 to 650 nm and from 570 nm to 700 nm) and two in the infrared region (from about 700 nm to 1400 nm and from 1400 nm to 2500 nm). Three of these four are reflected in the three major principal components (Figure 1B). The first and second principal components summarize the correlated features of the infrared spectrum, while the third corresponds to the major correlated features in the visible spectrum (Figure 1B).

Kalanchoe blossfeldiana, the only thick-leaved plant with CAM photosynthesis that we tested, is clearly distinguished from the rest by the first principal component. This species was characterized by a low reflectance around 1000 nm as well as in the intermediate infrared region. All other species investigated showed overlapping reflectance patterns, with no obvious correlation to structural components.

Partial Least Squares Regression with Recursive Feature Elimination Results in the Best Models for Photosynthetic Capacity

In order to find the model best suited for the prediction of photosynthetic capacity within a single species based on leaf reflectance data, we systematically tested a wide range of combinations of modeling algorithms and input transformations. The PCA analysis revealed that spectral features exhibit strong collinearity over a wide range of species, and we thus focused on methods with strong feature selection and used repeated cross-validation to find optimal parameters for each of these algorithms (Figure 2, see Methods). We found that neural networks perform similarly to partial least squares regression (PLSR) overall, but result in higher errors in specific cases (Figure 2). For example, PLSR results in significantly higher correlations (Pearson's R^2) between predicted and measured parameters for all outputs in *Brassica* and for the initial slope in *Zea* (adjusted $p < 7e^{-9}$ in each case). Using the first derivative of spectra instead of the raw data improved model performance for neural networks in all outputs in *Brassica* (adj. $p < 2e^{-10}$ in each case) but tended to decreased performance for PLSR models of CN ratio in both *Brassica* and *Zea* (adj. $p < 5e^{-7}$ in each case). Recursive feature elimination improved model performance in the case of A_{max} in *Brassica* (adj. $p < 0.04$) and for the initial slope in *Zea* (adj. $p < 8e^{-15}$). Model comparison on data for the close relative to *Brassica*, *Moricandia*, confirmed our findings in *Brassica* and *Zea* (Supplemental Figure 1). Based on these results, we decided to continue our analyses with a PLSR model with recursive feature selection that was trained on the original spectra without computing the first derivative.

We also estimated the effect of the choice of cross-validation method. In K-fold cross-validation, the data is partitioned into K random subsets. The prediction error is estimated by predicting the data in one subset based on a model trained on the remaining data. This approach is iterated over the K subsets and can be applied repeatedly. It is known that a bias-variance trade-off exists for the choice of K, where increasing K increases the variance of the error estimate but reduces its bias (Kohavi, 1995). We applied 20 times repeated K-fold cross-validation with different values for K, and a bias-variance trade-off was confirmed in the distributions of error estimates that resulted from our models (Supplemental Figure 1). We decided to use 5-fold cross-validation in the following analyses, as it provides a good balance between variance and pessimistic bias of the performance estimate.

Predictability Improvements Diminish after About 50 Samples but Tend to Be Species-Specific

The use of leaf spectral reflectance to estimate physiological parameters depends largely on the efficient generation of experimental data for model training. For large screening experiments, this will also be the most laborious and time-consuming part. To provide a guideline for the necessary amounts of data, we determined the number of samples that led to a saturation of model error reductions for different output parameters and species.

Learning curves are a valuable tool to check for the potential benefit that might result from obtaining additional data and to

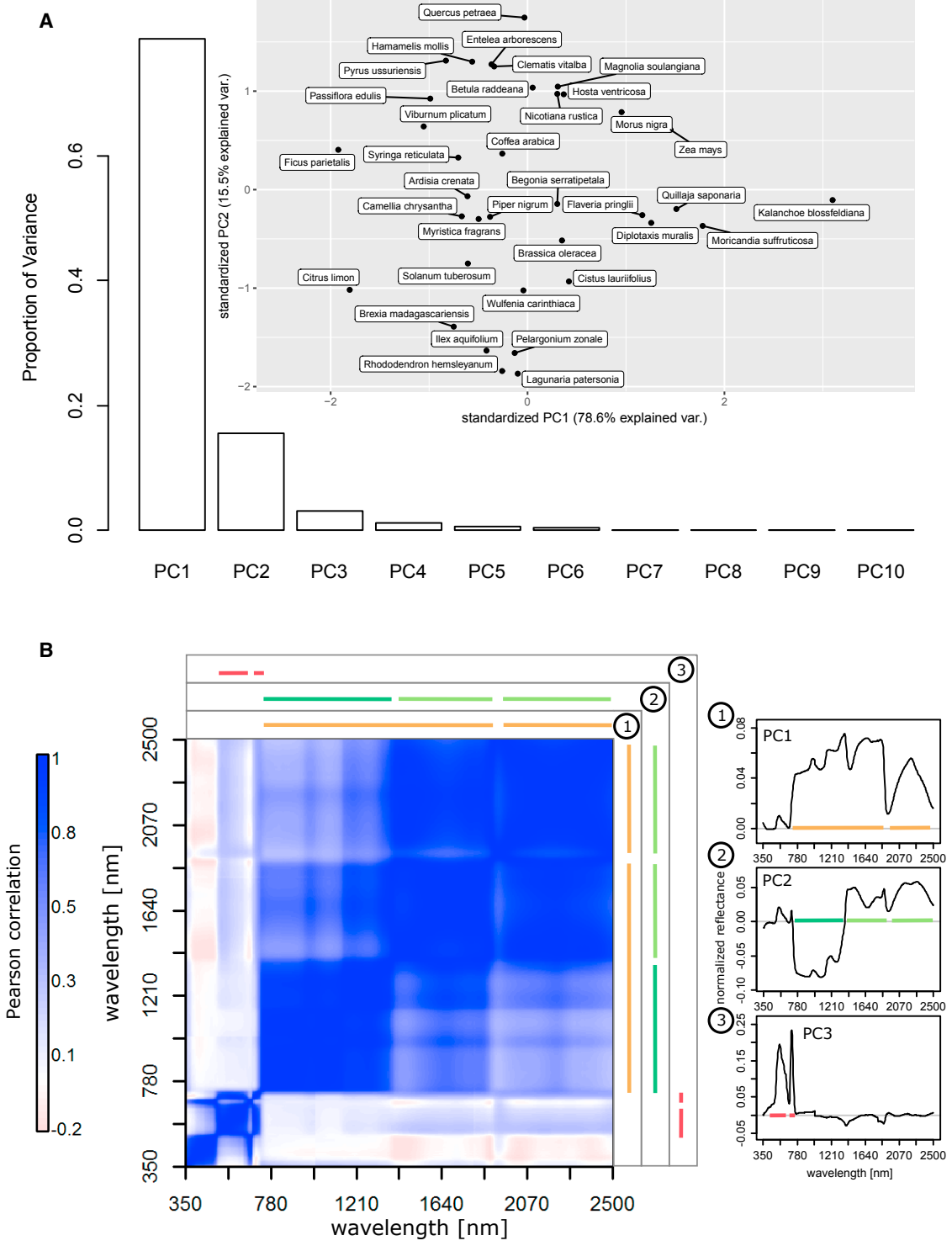

Figure 1. Properties of Leaf Reflectance over a Wide Range of Species.

(A) Proportion of variance covered by the first 10 principal components of reflectance spectra across 36 species. The inset shows a biplot that results from projecting the spectra onto the first and second component. Text labels are centered on the respective data point.

(B) Correlation heatmap of reflectance spectra in the 36 species. Each point shows the Pearson correlation of reflectance at the two respective wavelengths. The margins indicate correlated parts of the spectra and indicate which principal component contains this correlated area. Panels on the right show the three components that explain the highest proportion of variance. See also Supplemental Table 2.

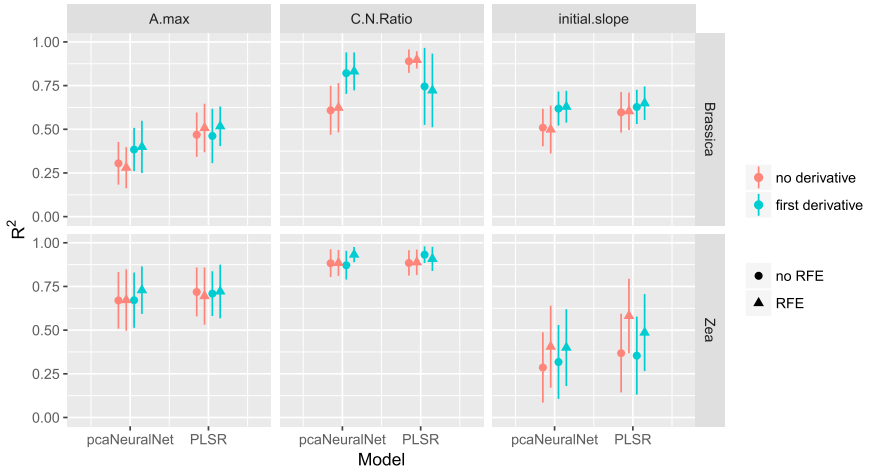

Figure 2. Correlation between Predicted and Measured Parameters across Models, Input Transformations, and Feature Selection Methods.

Circles indicate training with recursive feature elimination (RFE), triangles indicate training without RFE; red symbols indicate cases where no derivative of the input spectra was taken, while blue symbols show the use of the first derivative. See text for details on test statistics. Error bars correspond to the SD across repeated cross-validations. See also Supplemental Figure 1 and Supplemental Table 1.

spot problems with insufficient model complexity. The initial size of our dataset included about 40 individuals per genus. We calculated learning curves by training the models on sub-samples of the training sets, while keeping the size of the validation set constant. In the case of *Brassica*, this analysis revealed that the model could likely be improved by adding additional observations; we thus obtained additional samples for this species. The final learning curves reveal species-specific differences in the required number of observations (Figure 3). While *Brassica* requires about 70 samples to saturate the cross-validated error, *Zea* required little more than 30 samples (Figure 3). The error for the *Moricandia* species saturated at around 30 samples, similar to *Zea* (data not shown). These results point to an initial sample size of about 50 for future experiments, but learning curves should be examined to check for further gains through expanded sampling.

In all cases except for the CN ratio in *Zea*, the training error (i.e., the deviation between predictions and measurements within the training dataset) increases significantly above 30 samples (Figure 3). This indicates insufficient model complexity, but this effect is specific to the PLSR with recursive feature elimination (RFE). When RFE is not used, the training error is about zero, even for large samples (data not shown). Low model complexity in the form of a low number of features appears to benefit the generalizability of the predictions by avoiding overfitting (see Methods).

Photosynthetic Capacity within Species Can Be Predicted from Reflectance Spectra

When training the PLSR model with RFE on the full dataset for each species, the resulting models showed good performance for most species–output combinations (Table 1, Figure 4). The best predictions across all outputs were achieved for the CN ratio, with R^2 values of about 0.9. The crop plants *Brassica* and *Zea* exhibit inherent differences in photosynthetic machinery, since the former is a C_3 plant, while the latter conducts C_4 photosynthesis. The initial slope of the A-C_i curve will thus be associated with Rubisco content in *Brassica*, while it will tend to include the activity of PEPC and carbonic anhydrases as well as structural features influencing mesophyll conductance in the C_4 plant *Zea* (see Methods). Models for the initial slope selected strikingly different sets of features for C_3 species than for the C_4 species (Supplemental Figure 2), but we found that model performance was comparable in both species. This was not the case for the maximal photosynthetic rate A_{max}, where the model for *Zea* performed better than that for *Brassica* (adj. $p < 1e^{-13}$).

For C_3 species such as *Brassica oleraceae*, A-C_i curves can be used for the determination of the parameters V_{cmax} and J_{max}, which are directly connected to the photosynthetic performance of the leaf (Long and Bernacchi, 2003). V_{cmax} was calculated from the A-C_i curve at low CO_2 concentrations and shows a close relationship to the initial slope of the curve (R^2 = 0.88); J_{max} was calculated from the curve at saturating CO_2 concentrations and shows a close relationship to A_{max} (R^2 = 0.93). In *Brassica*, models trained for the prediction of the initial slope and A_{max} were very similar regarding the selected components and performance to the models of V_{cmax} and J_{max}, respectively (Supplemental Table 3, Supplemental Figure 5). The C_4 species are more complex because V_{cmax} and the maximum rate of phosphoenolpyruvate carboxylation (V_{pmax}) both influence the A-C_i curve (Massad et al., 2007). In the following, we therefore use the initial slope and A_{max} for characterization of photosynthesis in order to allow the use of the same parameters in C_3 as well as C_4 species and thus allow an unbiased comparison across photosynthetic types. In addition, this approach avoids an additional model fitting step that could introduce additional errors (Doughty et al., 2011).

Cross-Species Prediction Is Possible for Selected Traits

Our analysis of the spectral properties of leaves across a wide range of species indicated a low diversity of spectral properties (Figure 1). Based on this result, we were interested in the transferability of models across species domains. We thus mimicked the cross-validation procedure used for the intra-species models by replacing the validation subsets with data from a different species while using down-sampling to achieve training sets of equal sizes. This results in estimates of cross-species model performance that can be compared with that of the intra-species models.

The trait with the highest model transferability was the CN ratio, although the performance was significantly lower than for the intraspecific models (Supplemental Figure 3). The highest cross-species performance was found for predicting CN in *Zea* with models trained on *Brassica* (R^2 = 0.65) or *Moricandia*

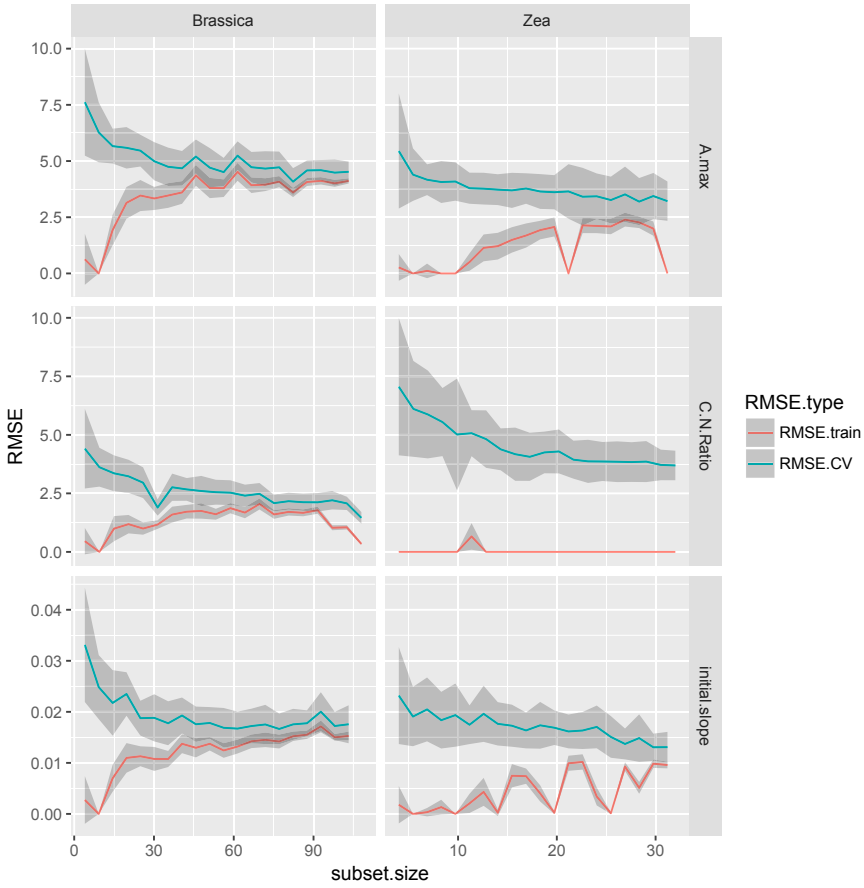

Figure 3. Learning Curves of PLSR models.
Blue line, root mean squared error (RMSE) estimated from K-fold cross-validation; red line, RMSE resulting from prediction of the training data. Gray shaded areas show the SD that results from the cross-validation procedure. The unit of RMSE is μmol s^{-1} m^{-2} for A_{max} and μmol s^{-1} m^{-2} ppm^{-1} for initial slope. See also Supplemental Table 1.

(R^2 = 0.66) (Supplemental Figure 3). Surprisingly, the transferability of CN ratio models between the two Brassicaceae genera *Moricandia* and *Brassica* was significantly lower, indicating that model transferability is not strictly related to phylogenetic proximity. Cross-species model performance for the two photosynthetic traits A_{max} and initial slope were strongly reduced compared with intra-species models, indicating that selected features are highly specific for the species the model is trained on (see Supplemental Figure 2).

Simulation of a Breeding Experiment Shows that Photosynthetic Capacity Can Be Improved Using Leaf Reflectance Data

Reflectance-based estimates could in principle be used to select for increased photosynthetic capacity in crops. In contrast to prediction of the CN ratio, models for the more complex traits A_{max} and initial slope were found to exhibit only moderately high prediction performance, and it is thus not clear whether the error of phenotyping is low enough to allow for efficient enrichment of photosynthetic capacity traits. In order to estimate the potential of our photosynthetic capacity models in the context of artificial selection, we simulated a breeding experiment. We simulated plant populations of each 1000 individuals for A_{max} and initial slope in *Brassica* and *Zea* as random draws from a normal population (see Methods for details). The mean of this distribution was set to the respective mean photosynthetic capacities we measured in this study and the SD to that found in wheat lines (Driever et al., 2014). We then simulated reflectance phenotyping of the 1000 individuals by adding random error as it was measured by our cross-validation procedure (Table 1) and selecting the best 10% of these "error-injected" phenotypes. This procedure was repeated 1000 times and the selection differential (i.e., the difference in mean phenotypic trait before and after selection) was recorded (Figure 5).

The simulation shows that both initial slope and A_{max} exhibit a strong response to selection based on leaf reflectance data and the models we trained (Figure 5). The response for the two crops *Zea* and *Brassica* is of similar magnitude, with *Zea* receiving slightly higher gains in A_{max} due to the more accurate prediction in this species. After this single round of selection, the average A_{max} in *Brassica* was increased by about 1.6 μmol m^{-2} s^{-1} (a relative gain of 6%) and by 1.8 μmol m^{-2} s^{-1} (7%) in *Zea*. The average initial slope in *Brassica* was enhanced by about 0.010 μmol m^{-2} s^{-1} ppm^{-1} (a relative gain of 9%) and by 0.011 μmol m^{-2} s^{-1} ppm^{-1} (10%) in *Zea*. These results suggest that high-throughput leaf reflectance measurements coupled with our regression models have the potential to become a highly efficient tool for the improvement of crop photosynthetic capacity through selective breeding.

DISCUSSION

The improvements in yield that drove the green revolution were mainly based on optimization of the harvest index, a trait that is now close to its theoretical maximum (Zhu et al., 2008; Amthor, 2010; Furbank and Tester, 2011). The largest margin of potential improvement now lies in the crop photosynthetic apparatus (Long et al., 2006). With the promises of synthetic biology still being hampered by the complexity of plant biology and legal boundaries, harnessing natural variation of photosynthetic machinery through breeding approaches is an auspicious route to enhanced crop yields. Gas exchange measurements still are cumbersome experimental techniques not suitable for large-scale phenotyping, and novel techniques are thus required to efficiently select for photosynthetic capacity. To establish an efficient phenotyping system for selective breeding for photosynthetic capacity, we studied the properties of leaf clip reflectance measurements and corresponding predictive models.

	A_{max} RMSE (SD) [No. of RFE Features, No. of PLS components]	A_{max} R^2 (SD)	CN RMSE (SD) [No. of RFE features, No. of PLS Components]	CN R^2 (SD)	Initial slope RMSE (SD) [No. of RFE features, No. of PLS Components]	Initial Slope R^2 (SD)
Brassica oleracea	3.99 (0.54) [10, 7]	0.51 (0.14)	1.34 (0.20) [100, 27]	0.90 (0.05)	0.016 (0.0026) [10, 9]	0.6 (0.11)
Zea mays	3.38 (0.95) [25, 4]	0.69 (0.16)	3.77 (0.97) [431, 3]	0.89 (0.07)	0.013 (0.0028) [10, 6]	0.58 (0.21)
Moricandia (mixed species)	4.89 (0.92) [10, 4]	0.44 (0.21)	2.34 (0.68) [100, 11]	0.80 (0.12)	0.019 (0.0050) [25, 7]	0.65 (0.18)

Table 1. Prediction Results of the PLSR Model with RFE on Raw Spectra.
Round brackets show the standard deviation of the performance estimate that results from repeated cross-validation. Square brackets indicate the number of features selected by the RFE procedure and the number of components used in the PLS algorithm. The unit of RMSE is $\mu mol\ s^{-1}\ m^{-2}$ for A_{max} and $\mu mol\ s^{-1}\ m^{-2}\ ppm^{-1}$ for initial slope; the CN ratio is dimensionless. See also Supplemental Figures 2 and 3.

In order to understand the general properties and diversity of leaf reflectance spectra, we estimated their distribution over a wide range of species. This revealed a surprisingly low diversity of spectral properties, indicating that robust, species-independent models to predict leaf properties might be obtainable with large datasets, a prospect especially promising for ecological research, where species-independent models would allow for the photosynthetic characterization of non-model species. This initial expectation was contrasted by our cross-species model evaluation (Supplemental Figure 3). We found that model transfer leads to much higher errors than in the intra-species predictions. Furthermore, transferability cannot be predicted by phylogenetic relatedness, as shown by the finding that transferability from *Moricandia* to *Brassica*, two closely related Brassicaceae species, is generally not higher than between *Zea mays* and *Brassica*. Our results thus confirm the superiority of species-specific models (Yendrek et al., 2017).

The analysis of a diverse array of leaf spectra revealed major ranges of wavelengths in which leaf reflectance was highly correlated. This feature of the spectra poses a problem for the development of robust predictive models, because preference of certain wavelengths might be purely due to measurement noise in the many similar features that are measured. On the other hand, the highly correlated areas in crop reflectance spectra might provide an opportunity for the development of more cost-efficient phenotyping devices, because a high-resolution measurement across the whole 350–2500 nm range might not be necessary to predict specific phenotypic traits of interest.

In order to develop prediction models with high precision, we systematically evaluated the performance of a variety of models. Past studies on predicting various plant traits on leaf reflectance data used simple ratios of reflectance at two or three wavelengths (Zhao et al., 2005; Wang et al., 2012b), PLS with different pretreatments (Ourcival et al., 1999; Serbin et al., 2012; Ecarnot et al., 2013), and neural networks (Liu et al., 2010b); but systematic studies of a wide range of algorithms are to our knowledge not available. Based on the strong correlation among most of the features (Figure 1), we focused on methods designed to deal with the problem of collinearity. We optimized a variety of combinations of preprocessing and prediction model, whether we take the first derivative or not, use or omit recursive feature selection, and employ non-linear neural networks or linear PLSR, to find the algorithm most suitable for predicting crop photosynthesis. Although many algorithms yielded similar performance as measured by RMSE and R^2, PLSR with RFE without using the derivatives of spectra resulted in significantly superior prediction performance across model outputs and species. This result indicates that the potential of learning non-linear mappings in neural networks is not required for predicting photosynthetic capacity, at least with moderately sized datasets. Although PLSR is in itself designed to reduce the number of predictors, RFE improved its performance in selected cases by adding an additional layer of feature selection.

We further used learning curves to gradually adapt the size of the training datasets (Figure 3). While cross-validated model errors saturated with sample size at around 30 observations in *Zea* and *Moricandia*, models on *Brassica* benefitted from additional samples and saturated only at around 70 samples. These observations allow us to recommend initial sample sizes of at least 50 observations for future experiments on novel species, but also suggest the use of learning curves to ensure that no further performance gain can be obtained from additional experiments.

Interestingly, the training error clearly approaches the cross-validated error in many species–output combinations, indicating that model bias is limiting further improvement in prediction error. We found this lack of model complexity to be the result of the RFE (data not shown), suggesting that the low complexity serves model robustness by avoiding overfitting.

Using the selected training algorithm, we found that the CN ratio was the parameter resulting in the highest correlation between predictions and observations, with R^2 of about 0.9 for *Brassica* and *Zea* (Table 1). The nitrogen status is a parameter commonly estimated based on leaf reflectance data (Alchanatis et al., 2005; Zhao et al., 2005; Serbin et al., 2012), and the good performance of our models on this parameter served as a control for our experimental system. In terms of features selected for leaf nitrogen predictions, earlier studies have used spectral indices composed of reflectance at only two to three wavelengths, mostly in the blue, green, and near infrared region (Rodriguez et al., 2006; Yao et al., 2010; Wang et al., 2012b). Interestingly, our models selected a wide range of spectra (210 features on average) to predict the CN ratio, with a clear focus on the visible region only present in *Zea*. Since we actively counteract overfitting by allowing the model selection procedure to sacrifice prediction performance for the sake of

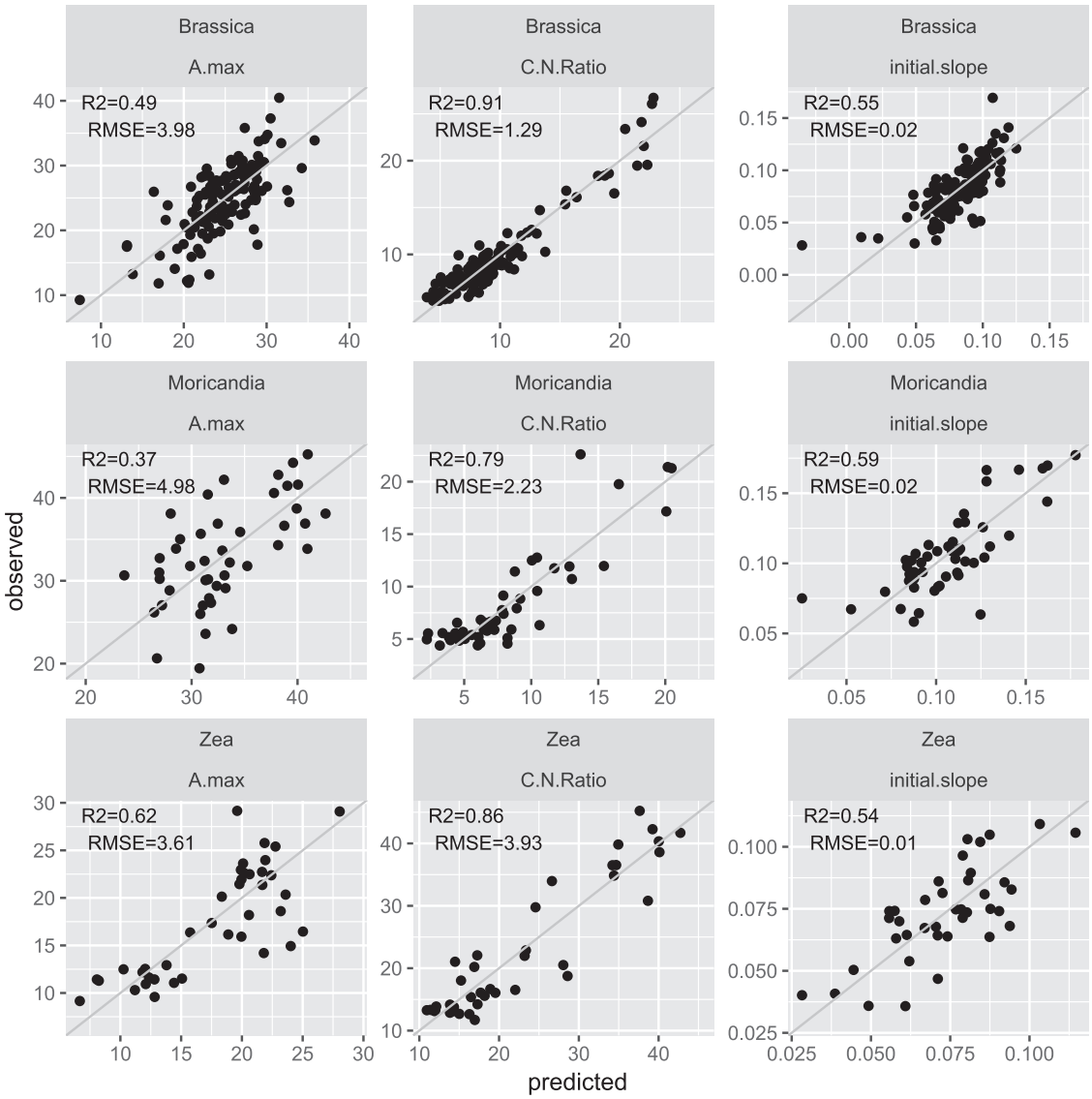

Figure 4. Example Predictions of the Validation Set during a Randomly Chosen Iteration of Repeated Cross-Validation.

models that use fewer features (see Methods), and a high number of features were selected consistently across species, this high model complexity appears to be required for predicting the CN ratio accurately.

Prediction of the parameters for photosynthetic capacity (initial slope of the A-C_i curve and maximal photosynthetic rate A_{max}) yielded high correlations between predictions and observations, albeit not as high as in the case of the CN ratio (Table 1). A possible reason for this discrepancy lies in the higher complexity of these traits, with multiple components contributing to both A_{max} and initial slope. Interestingly, we found significant differences between *Zea* and *Brassica* in models for A_{max}, where models for *Zea* were more accurate than those for *Brassica*. The interpretation of A_{max} has to differ between C_3 and C_4 plants, since maximal ribulose-1,5-bisphosphate (RuBP) regeneration capacity is based on the interaction between mesophyll and bundle sheath cells in maize (Majeran and van Wijk, 2009) and this might be a reason for the difference in performance. As photosynthetic capacity will be tied to the proteins in the Calvin Benson cycle, the C_4 cycle, and the light reactions, it will in some cases be tied to leaf nitrogen concentration. To investigate whether the performance of our models might be based on a spectra-based estimation of leaf nitrogen content, we analyzed correlations between our parameters for photosynthetic capacity and the CN ratio. We found a strong correlation between A_{max} and CN ratio in *Zea* (R^2 = 0.65, Supplemental Table 1) that was not present for *Moricandia* (R^2 = 0.07) and *Brassica* (R^2 = 0.006). This apparent nitrogen-dependence of A_{max} might explain the superior performance of A_{max} models in *Zea* by the good performance of models for the CN ratio. In agreement with this reasoning, selected features are similar in A_{max} and CN ratio models for *Zea*, but not for the other species (Supplemental Figure 2). In a similar setup, Yendrek et al. (2017) could also show strong correlation between an LRS-based model and maximal photosynthetic capacity of *Zea mays* under saturating CO_2 concentrations. Their model shows very high correlation between maximal

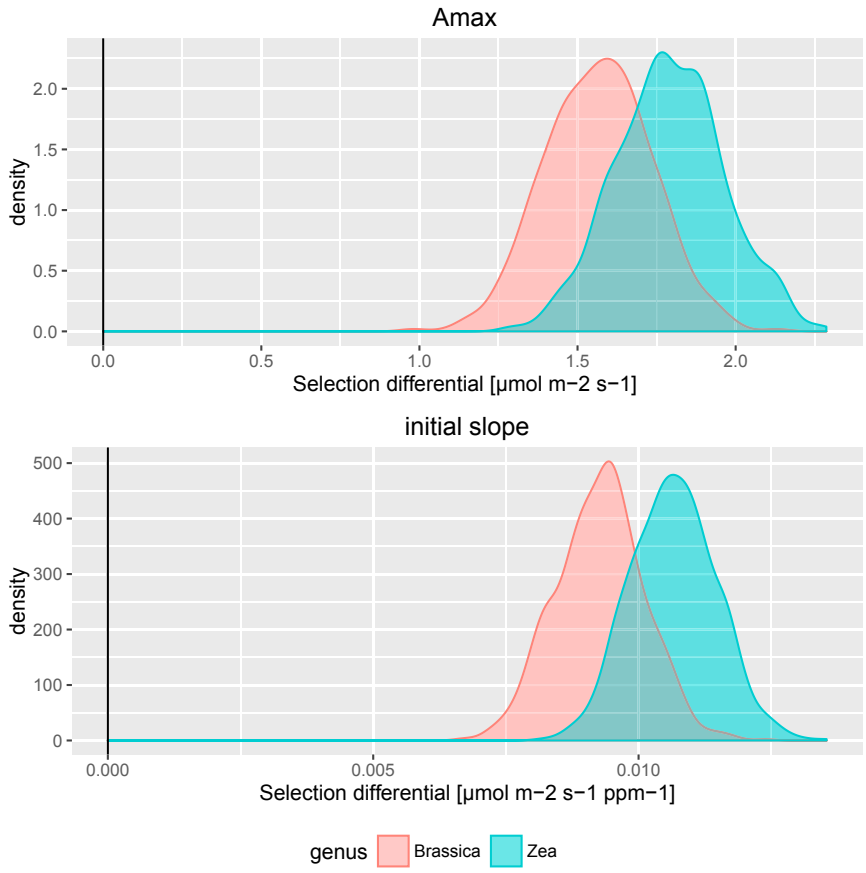

Figure 5. Simulated Responses to Selection.
Distribution of selection differential (the difference between mean traits in the original and selected population) for A_{max} and initial slope is shown after 1000 simulations of an experiment where 10% of a parent population were phenotyped and selected using leaf reflectance measurements. The phenotyping error was set to the cross-validated RMSE and assumed to be normally distributed. The relative gain in A_{max} in *Brassica* and *Zea* is about 6% and 7%, respectively. The relative gain in initial slope in *Brassica* and *Zea* is about 9% and 10%, respectively. See Supplemental Figure 4 and text for details.

assimilation capacity and chlorophyll content of the leaves. When comparing the selected features for our models of A_{max} with published indices used for chlorophyll estimation (Datt, 1998; le Maire et al., 2004; Maccioni et al., 2001; Sims and Gamon, 2002; Vogelmann et al., 1993), we found a much stronger overlap in the *Zea* model than in the C_3 species (Supplemental Figure 3). In agreement with this finding, most of the indices predict A_{max} in *Zea* with high accuracy (average R^2 = 0.65, Supplemental Table 2). Interestingly, this is not the case for the C_3 species (average R^2 = 0.09).

Features for the models of initial slope were found exclusively in the visible spectrum, and striking similarities can be seen between the features selected in models of *Brassica* and *Moricandia*, especially at 600 and around 525 nm (Supplemental Figure 2). Serbin et al. (2012) report features that are used to predict maximum rates of RuBP carboxylation (V_{cmax}) in *Populus* trees, a quantity that should be correlated with the initial slope, at least in the C_3 plant *Brassica*. While their model also focused on the visible region and selected features in the 600 nm region, many features of the infrared region were included. In the experimental setup of Yendrek et al. (2017), the activity of PEPC (V_{pmax}) was calculated from the initial part of the A-C_i curve of C_4 maize leaves, but accurate prediction of V_{pmax} by PLSR models from LRS data was not possible. In our experiment, the prediction of the initial slope in the A-C_i curve of *Zea mays* was also less powerful than for prediction of A_{max} in the same species. In contrast to A_{max}, the relationship between the initial slope and CN ratio was much weaker (Supplement Table 1), suggesting that the initial slope models were not based on measuring leaf nitrogen content. In agreement with this finding, published chlorophyll indices showed only weak performance in predicting the initial slope in all species (Supplemental Table 3).

In an ecological setting, models for the prediction of the maximal rate of photosynthetic electron transport and Rubisco content from leaf reflectance measurements were built for *Populus* trees, resulting in high correlations between predictions and observations (R^2 of about 0.9 for both outputs) (Serbin et al., 2012). These parameters are similar to the ones measured in this study, and the estimated error of these tree models is apparently lower than the one we estimated for *Brassica* and *Zea*. One reason for this discrepancy lies in differences in cross-validation methods; Serbin et al., 2012 used leave-one-out cross-validation, which suffers from high variance (also see Ecarnot et al., 2013), but lacks a pessimistic bias that is inherent to the 5-fold cross-validation used in this study (Kohavi, 1995) (Supplemental Figure 1). In addition, photosynthetic capacity varies drastically with leaf number and age in annual crops, an effect that is probably less drastic in deciduous trees where all leaves are formed at the same time in spring.

Models for the PS-related features generally did not reach the same accuracy as models that predict CN, and the overlap of the selected features also indicated that the variation in the N content was partly responsible for the variation in the predicted PS-related features, especially A_{max} in *Zea mays*. In addition, the content of specific chemical components of the leaf such as pigments and proteins as well as structural features such as leaf thickness could be detected by LRS and are likely to influence the models of the PS-related features. Especially, the model of A_{max} showed a strong overlay of chlorophyll-specific indices in all tested species (Supplemental Figure 3), indicating a generally strong dependency of A_{max} on chlorophyll content (Yendrek et al., 2017). Unknown features influencing LRS and further features possibly not detectable by LRS can be further responsible for the photosynthetic capacity of each genotype

under specific environmental conditions, and further experiments will be necessary for in-depth investigation of all underlying mechanisms. The results presented show, however, that LRS possesses sufficient accuracy for exploration of PS features in different environmental and genotypic backgrounds. The fast and non-destructive nature of the method will allow the selection of genotype/environment combinations with the greatest variance in PS capacity for more laborious in-depth experiments. LRS data obtained with the leaf clip is generally highly standardized and will allow high comparability of results from different studies, and increasing amount of available data can be used for improved models and new correlation analysis.

In order to estimate the models' applicability in selective breeding for photosynthetic capacity, we simulated 1000 breeding experiments that used reflectance spectra for phenotyping. The error of the method in these simulations was set to the RMSE that resulted from the cross-validation procedures (Table 1). We found significant selection differential for both initial slope and A_{max} in *Brassica* and *Zea*, showing that the performance of the method is high enough to improve each A_{max} and the initial slope in all 1000 cases (Figure 5). Although incomplete heritability will further mitigate the benefit for the next generation and variability in photosynthetic traits had to be estimated based on data from wheat, this result shows that leaf reflectance spectra can serve as a valuable tool for the improvement of crop photosynthetic capacity. Exploiting the high genetic variability in maize MAGIC lines for this purpose appears particularly promising. In addition to selective breeding, genetic mapping approaches based on reflectance phenotyping would enable understanding and utilization of the genomic variation underlying photosynthetic capacity.

We emphasize that we advocate leaf reflectance spectroscopy as a rapid first-pass screen to uncover variation in photosynthetic parameters in hundreds or thousands of genetically diverse individuals. Promising lines displaying variation would then have to be validated by more precise methods, such as infrared gas exchange analyzers. Given appropriate training of the prediction models, leaf reflectance spectroscopy can provide additional information beyond photosynthetic parameters such as the CN ratio, leaf water contents, and other important traits, which will allow for rapid deep-content first-pass phenotyping with a single device and the discovery of correlations between traits.

METHODS

Plant Material

General variation in leaf reflectance spectra of species from 36 different genera was measured on plants growing in the greenhouses and outdoor area of the Botanical Garden of the Heinrich-Heine University in Düsseldorf (Germany) during the summer months of 2015. These included leaves from trees, bushes, and herbaceous plants and covered both perennials and annuals (see Supplemental Table 2).

Two crop species, the dicotyledonous C_3 plant *Brassica oleracea* (var. "Grüner Ring", N.L. Chrestensen, Erfurt) and the monocotyledonous C_4 plant *Zea mays* (var. B73) were chosen for combined physiological measurements. Seeds were germinated on filter paper and transferred to pots filled with sand after 3–5 days. Plants were cultivated in the greenhouse of the university during the summer months of 2014 and 2015. The different nitrogen regimes were realized by watering every third day with a modified Hoagland solution. For maize and *Brassica*, the control or 100% N treatment consisted of 15 mM KNO_3, 5 mM $CaCl_2$, 2 mM $MgSO_4$, 2 mg/l Fe, 0.5 mM KH_2PO_4, 50 μM H_3BO_4, 10 μM $MnCl_2$, 1 μM $ZnSO_4$, 0.3 μM $CuSO_4$, and 0.5 μM Na_2MoO_4. For low N treatment, the KNO_3 content was reduced accordingly, and the differences in potassium supply were balanced with KCl. In the first year, plants of both species were cultivated under 100% and 10% N conditions resulting in 50 datasets from each species. In order to investigate whether models could be improved by higher sample number and better spread of data, the experiment was repeated with *Brassica oleraceae* plants fertilized with 100%, 50%, 30%, and 10% N. Measurements of gas exchange and leaf optical reflectance took place 4–5 weeks after germination. Close wild relatives of *Brassica oleraracea* from the genus *Moricandia* (*M. moricandioides, M. arvensis, M. suffruticosa)* were selected for comparable physiological and reflectance studies. *M. moricandoides* performs C_3 photosynthesis, while *M. arvensis and M. suffruticosa* are C_3–C_4 intermediate species. The plants were grown in a mixture of sand and soil and investigated 8–10 weeks after germination.

Leaf Optical Properties

We used the ASD FieldSpec4 High Res instrument for reflectance measurements. For the plants in the Botanical Garden, the instrument was switched on at least 1 h before use in the portable setup. Before each measurement, the instrument was calibrated by dark current and white reflectance adjustments. Leaf reflectance data covering the spectrum from 350 to 2500 nm in 1 nm steps were collected using the leaf clip from the adaxial side of mature leaves. Each scan represents the average of 10 passes. The total measuring time per leaf was less than 1 min and three technical replicate spectra were averaged for each plant.

In the greenhouse experiments, *Brassica* and *Moricandia* leaves at least 5 cm in length were analyzed. In maize, leaves were used when at least 20 cm had emerged, and only the upper third of the leaf was used, so that all studied material represented source leaf characteristics. The optical properties of the selected leaf parts were taken as described above before and after the gas exchange analysis. Ten biological replicates were used per experiment, N treatment, and species.

Gas Exchange Measurements

Immediately after the spectral reflectance scan, the selected part of the leaf was placed into the cassette of the LICOR 6400XT gas analyzer. The cuvette conditions were maintained at a photon flux of 1500 μmol m^{-2} s^{-1}, a block temperature of 25°C, and a flow rate of 300 mmol s^{-1}. After an adjustment period of approximately 15 min, A-C_i curves were obtained by stepwise changes in the external CO_2 supply ranging from 50 to 2000 ppm. The linear part of the A-C_i curve between 0 and 200 ppm ci was used for the calculation of the initial slope.

The interpretation of the slope of A-C_i curves differs between C_3 and C_4 plants. The initial slope is related to photosynthetic capacity in both C_3 and C_4 plants, but the underlying biochemical interpretations vary (von Caemmerer, 2000):

$$\frac{dA_{C3}}{dC_i} = \frac{g_i(V_{cmax} - A_{C3})}{(g_i(C_i + K_c(1 + O/K_o)) + V_{cmax} - 2A_{C3})}$$

$$\frac{dA_{C4}}{dC_i} = \frac{g_i V_{pmax}}{g_i K_p + V_{pmax}}$$

Where A_{C3} and A_{C4} are the net carbon assimilation rates in C_3 and C_4 plants, respectively; g_i is the intercellular conduction; V_{cmax} and V_{pmax} are the maximal activity of Rubisco and PEPC, respectively; ci is the intercellular CO_2 partial pressure; K_c and K_o are the Michaelis constants of Rubisco for CO_2 and O_2, respectively; and K_p is the Michaelis constant of PEPC for bicarbonate.

We used the initial slope of the A-C_i curve and the maximal assimilation rate at high CO_2 concentrations (A_{max}) as the two parameters to represent photosynthetic capacity in C_3 as well as C_4 plants. For the C_3 plant *Brassica*, the photosynthetic parameters V_{cmax} and J_{max} were additionally calculated using the "plantecophys" R package (Duursma, 2015) and compared with the parameters directly obtained from the A-C_i curve, i.e., initial slope and A_{max}, respectively. Use of the parameters initial slope and A_{max} allowed comparable data handling for the C_3 and C_4 species.

Determination of Leaf Nitrogen Content

After completion of the A-C_i curve, the selected leaf part was harvested and dried at 70°C for ca. 48 h. The material was then homogenized to a fine powder in a Mixer Mill MM301 (Retsch GmbH, Germany) for 1 min and analyzed using an Isoprime 100 isotope ratio mass spectrometer coupled to an ISOTOPE cube elemental analyzer (both from Elementar, Hanau, Germany) according to Gowik et al. (2011).

Model Training

In order to reduce computational complexity, the resolution of the reflectance spectra was reduced to 5 nm steps by discarding intermediate measurements. Technical replicates of spectra were averaged. Model training and parameter fitting was conducted by 20 times repeated K-fold cross-validation. The choice of K is subject to a bias-variance trade-off (see Supplemental Figure 1), and we decided on a K of 5, unless mentioned otherwise. Model training was implemented using the caret package of the R environment (Kuhn, 2016; R Development Core Team, 2015). In order to select the model that performs best on photosynthetic capacity outputs, we varied whether we used raw measurements or derivatives, whether we employed RFE, and what kind of model was trained. Statistical comparisons of performance measures were conducted using Wilcoxon rank sum tests, correcting for multiple testing (Benjamini and Hochberg, 1995). Note that the result of such tests is difficult to interpret statistically, since cross-validated samples are not independent. We visually compared resampling distributions to avoid type I errors due to sample dependence.

Partial Least Squares Regression

Partial least squares regression (PLSR) reduces the number of input features by projecting both the input and output data to latent components that maximize the product of squared input–output correlation with the variance of the projected data. The number of major components the data is projected onto was selected so as to minimize the root mean squared error (RMSE) as assessed through the cross-validation procedure described above. This parameter was chosen from the natural numbers of 1–50 (or the maximal number of components allowed by the size of the training set).

Neural Networks

Neural networks were trained to account for non-linear effects that might not be modeled by PLSR. We chose a shallow network of one hidden layer from the nnet package in R (Venables and Ripley, 2002). The number of neurons in the hidden layer was chosen by cross-validation from the following set: {1, 5, 20, 45}. In addition, the regularization parameter (decay) was fitted on a logarithmic scale: $\{1e^1, 1e^0, 1e^{-1}, 1e^{-2}, 1e^{-3}\}$. Input data was transformed by PCA, utilizing the smallest number of components that together accounted for at least 99% of the variance.

Recursive Feature Elimination

Since the data has far more features than observations, we employed RFE to obtain a set of valuable features. In RFE, the number of features is repeatedly reduced to the s_i most important features, starting with the full set of features s_1. In each iteration, the model was re-trained on the s_i remaining features. We chose $\{s_1, \ldots, s_n\}$ to be {10, 15, 20, 25, 50, 100, 431}. Feature importance was evaluated by the cross-validation procedure detailed above in combination with the standard methods for neural networks and PLSR of the caret package. The optimal parameter (i.e., number of features) was chosen to be the smallest number of features that does not exceed the smallest RMSE found by more than 5%. This criterion was chosen to obtain simple models that are less likely to be prone to overfitting. Problems with overfitting are further counteracted by external cross-validation of the RFE procedure itself in addition to the cross-validation used to tune the model parameters described above.

Simulation of Artificial Selection

In order to estimate the potential benefit of the trained reflectance-based models for improving crops in this way, we simulated a selective breeding experiment that uses leaf reflectance spectra for phenotyping. We used published data on the natural variability of photosynthetic capacity in wheat lines (Driever et al., 2014) to estimate possible variation of photosynthetic capacity in a population of 1000 *Zea* or *Brassica* plants. A_{max} and initial slope were further assumed to be normally distributed in agreement with the situation in wheat (Driever et al., 2014), with mean trait values set to the species means observed in our experiments. We found the model prediction errors to be normally distributed (Supplemental Figure 4) and thus used an additive normally distributed error with the SD estimated by the cross-validated RMSE (Table 1). To estimate the distribution of potential gain resulting from selecting 10% of the population, we simulated the experiment 1000 times and recorded the selection differential (i.e., the difference in mean phenotypic trait before and after selection).

SUPPLEMENTAL INFORMATION

Supplemental Information is available at *Molecular Plant Online*.

FUNDING

We acknowledge financial support by the Deutsche Forschungsgemeinschaft (grants IRTG 1525, SPP 1529, and EXC 1208) and the German Federal Ministry of Research and Education (BMBF, grant 031B0205A).

AUTHOR CONTRIBUTIONS

U.S. conducted the experiments; D.H. conducted data analysis and modeling; D.H., U.S., and A.P.M.W. designed the research and wrote the paper.

ACKNOWLEDGMENTS

The authors would like to thank David M. Kramer, Martin J. Lercher, and Benjamin Stich for their insightful comments on the manuscript and Roselane Kithan for technical assistance during spectral reflectance measurements in the Botanical Garden of the Heinrich Heine University in Düsseldorf. No conflict of interest declared.

Received: March 21, 2017
Revised: March 21, 2017
Accepted: April 23, 2017
Published: April 28, 2017

REFERENCES

Ainsworth, E.A., Serbin, S.P., Skoneczka, J.A., and Townsend, P.A. (2014). Using leaf optical properties to detect ozone effects on foliar biochemistry. Photosynth. Res. **119**:65–76.

Alchanatis, V., Schmilovitch, Z., and Meron, M. (2005). In-field assessment of single leaf nitrogen status by spectral reflectance measurements. Precision Agric. **6**:25–39.

Amthor, J.S. (2010). From sunlight to phytomass: on the potential efficiency of converting solar radiation to phyto-energy. New Phytol. **188**:939–959.

Atzberger, C., Guerif, M., Baret, F., and Werner, W. (2010). Comparative analysis of three chemometric techniques for the spectroradiometric assessment of canopy chlorophyll content in winter wheat. Comput. Electron. Agr. **73**:165–173.

Baker, N.R. (2008). Chlorophyll fluorescence: a probe of photosynthesis in vivo. Annu. Rev. Plant Biol. **59**:89–113.

Bandillo, N., Raghavan, C., Muyco, P.A., Sevilla, M.A.L., Lobina, I.T., Dilla-Ermita, C.J., Tung, C.W., McCouch, S., Thomson, M., Mauleon, R., et al. (2013). Multi-parent advanced generation inter-cross (MAGIC) populations in rice: progress and potential for genetics research and breeding. Rice (NY) **6**:11.

Bao, Y.S., Xu, K., Min, J.Z., and Xu, J.J. (2013). Estimating wheat shoot nitrogen content at vegetative stage from in situ hyperspectral measurements. Crop Sci. **53**:2063–2071.

Benjamini, Y., and Hochberg, Y. (1995). Controlling the false discovery rate - a practical and powerful approach to multiple testing. J. Roy. Stat. Soc. B Met. **57**:289–300.

Borregaard, T., Nielsen, H., Norgaard, L., and Have, H. (2000). Crop-weed discrimination by line imaging spectroscopy. J. Agr. Eng. Res. **75**:389–400.

Couture, J.J., Serbin, S.P., and Townsend, P.A. (2013). Spectroscopic sensitivity of real-time, rapidly induced phytochemical change in response to damage. New Phytol. **198**:311–319.

Datt, B. (1998). Remote sensing of chlorophyll a, chlorophyll b, chlorophyll a+b, and total carotenoid content in eucalyptus leaves. Remote Sens. Environ. **66**:111–121.

Dell'Acqua, M., Gatti, D.M., Pea, G., Cattonaro, F., Coppens, F., Magris, G., Hlaing, A.L., Aung, H.H., Nelissen, H., Baute, J., et al. (2015). Genetic properties of the MAGIC maize population: a new platform for high definition QTL mapping in Zea mays. Genome Biol. **16**:167.

Dillen, S.Y., Op de Beeck, M., Hufkens, K., Buonanduci, M., and Phillips, N.G. (2012). Seasonal patterns of foliar reflectance in relation to photosynthetic capacity and color index in two co-occurring tree species, *Quercus rubra* and *Betula papyrifera*. Agr. For. Meteorol. **160**:60–68.

Doughty, C.E., Asner, G.P., and Martin, R.E. (2011). Predicting tropical plant physiology from leaf and canopy spectroscopy. Oecologia **165**:289–299.

Driever, S.M., Lawson, T., Andralojc, P.J., Raines, C.A., and Parry, M.A.J. (2014). Natural variation in photosynthetic capacity, growth, and yield in 64 field-grown wheat genotypes. J. Exp. Bot. **65**:4959–4973.

Duursma, R.A. (2015). Plantecophys - an R package for analysing and modelling leaf gas exchange data. PLoS One **10**:e0143346.

Ecarnot, M., Compan, F., and Roumet, P. (2013). Assessing leaf nitrogen content and leaf mass per unit area of wheat in the field throughout plant cycle with a portable spectrometer. Field Crops Res. **140**:44–50.

Fiorani, F., and Schurr, U. (2013). Future scenarios for plant phenotyping. Annu. Rev. Plant Biol. **64**:267–291.

Furbank, R.T., and Tester, M. (2011). Phenomics - technologies to relieve the phenotyping bottleneck. Trends Plant Sci. **16**:635–644.

Gillon, D., Houssard, C., and Joffre, R. (1999). Using near-infrared reflectance spectroscopy to predict carbon, nitrogen and phosphorus content in heterogeneous plant material. Oecologia **118**:173–182.

Gowik, U., Bräutigam, A., Weber, K.L., Weber, A.P.M., and Westhoff, P. (2011). Evolution of C_4 photosynthesis in the genus *Flaveria*: how many and which genes does it take to make C_4? Plant Cell **23**:2087–2105.

Harbinson, J. (2013). Improving the accuracy of chlorophyll fluorescence measurements. Plant Cell Environ. **36**:1751–1754.

Harbinson, J., Prinzenberg, A.E., Kruijer, W., and Aarts, M.G.M. (2012). High throughput screening with chlorophyll fluorescence imaging and its use in crop improvement. Curr. Opin. Biotechnol. **23**:221–226.

Jia, F.F., Liu, G.S., Ding, S.S., Yang, Y.F., Fu, Y.P., and Wang, Z.H. (2013). Using leaf spectral reflectance to monitor the effects of shading on nicotine content in tobacco leaves. Ind. Crops Prod. **51**:444–452.

Kira, O., Nguy-Robertson, A.L., Arkebauer, T.J., Linker, R., and Gitelson, A.A. (2016). Informative spectral bands for remote green LAI estimation in C_3 and C_4 crops. Agr. For. Meteorol. **218**:243–249.

Kohavi, R. (1995). A study of cross-validation and bootstrap for accuracy estimation and model selection. In IJCAI'95 Proceedings of the 14th International Joint Conference on Artificial Intelligence, *Volume 2* (San Francisco, CA: Morgan Kaufmann), pp. 1137–1145.

Kromdijk, J., and Long, S.P. (2016). One crop breeding cycle from starvation? How engineering crop photosynthesis for rising CO_2 and temperature could be one important route to alleviation. Proc. Biol. Sci. **283**:20152578.

Kuhn, M. (2016). Caret: Classification and Regression Training, Available online at: http://topepo.github.io/caret/index.html.

le Maire, G., Francois, C., and Dufrene, E. (2004). Towards universal broad leaf chlorophyll indices using PROSPECT simulated database and hyperspectral reflectance measurements. Remote Sens. Environ. **89**:1–28.

Liu, Y.L., Chen, H., Wu, G.F., and Wu, X.G. (2010a). Feasibility of estimating heavy metal concentrations in *Phragmites australis* using laboratory-based hyperspectral data-A case study along Le'an River, China. Int. J. Appl. Earth Obs. **12**:S166–S170.

Liu, Z.Y., Wu, H.F., and Huang, J.F. (2010b). Application of neural networks to discriminate fungal infection levels in rice panicles using hyperspectral reflectance and principal components analysis. Comput. Electron. Agr. **72**:99–106.

Long, S.P., and Bernacchi, C.J. (2003). Gas exchange measurements, what can they tell us about the underlying limitations to photosynthesis? Procedures and sources of error. J. Exp. Bot. **54**:2393–2401.

Long, S.P., Zhu, X.G., Naidu, S.L., and Ort, D.R. (2006). Can improvement in photosynthesis increase crop yields? Plant Cell Environ. **29**:315–330.

Long, S.P., Marshall-Colon, A., and Zhu, X.G. (2015). Meeting the global food demand of the future by engineering crop photosynthesis and yield potential. Cell **161**:56–66.

Maccioni, A., Agati, G., and Mazzinghi, P. (2001). New vegetation indices for remote measurement of chlorophylls based on leaf directional reflectance spectra. J. Photochem. Photobiol. B **61**:52–61.

Mackay, I.J., Bansept-Basler, P., Barber, T., Bentley, A.R., Cockram, J., Gosman, N., Greenland, A.J., Horsnell, R., Howells, R., O'Sullivan, D.M., et al. (2014). An eight-parent multiparent advanced generation inter-cross population for winter-sown wheat: creation, properties, and validation. G3 (Bethesda) **4**:1603–1610.

Mahlein, A.K., Oerke, E.C., Steiner, U., and Dehne, H.W. (2012). Recent advances in sensing plant diseases for precision crop protection. Eur. J. Plant Pathol. **133**:197–209.

Majeran, W., and van Wijk, K.J. (2009). Cell-type-specific differentiation of chloroplasts in C_4 plants. Trends Plant Sci. **14**:100–109.

Manevski, K., Manakos, I., Petropoulos, G.P., and Kalaitzidis, C. (2011). Discrimination of common Mediterranean plant species using field spectroradiometry. Int. J. Appl. Earth Obs. **13**:922–933.

Massad, R.S., Tuzet, A., and Bethenod, O. (2007). The effect of temperature on C_4-type leaf photosynthesis parameters. Plant Cell Environ. **30**:1191–1204.

Maurino, V.G., and Weber, A.P.M. (2013). Engineering photosynthesis in plants and synthetic microorganisms. J. Exp. Bot. **64**:743–751.

Murchie, E.H., and Lawson, T. (2013). Chlorophyll fluorescence analysis: a guide to good practice and understanding some new applications. J. Exp. Bot. **64**:3983–3998.

Ort, D.R., Merchant, S.S., Alric, J., Barkan, A., Blankenship, R.E., Bock, R., Croce, R., Hanson, M.R., Hibberd, J.M., Long, S.P., et al. (2015). Redesigning photosynthesis to sustainably meet global food and bioenergy demand. Proc. Natl. Acad. Sci. USA **112**:8529–8536.

Ourcival, J., Joffre, R., and Rambal, S. (1999). Exploring the relationships between reflectance and anatomical and biochemical properties in *Quercus ilex* leaves. New Phytol. **143**:351–364.

Penning, B.W., Hunter, C.T., Tayengwa, R., Eveland, A.L., Dugard, C.K., Olek, A.T., Vermerris, W., Koch, K.E., McCarty, D.R., Davis, M.F., et al. (2009). Genetic resources for maize cell wall biology. Plant Physiol. **151**:1703–1728.

R Development Core Team. (2015). R: A Language and Environment for Statistical Computing, https://www.r-project.org/.

Rodriguez, D., Fitzgerald, G., Belford, R., and Christensen, L. (2006). Detection of nitrogen deficiency in wheat from spectral reflectance indices and basic crop eco-physiological concepts. Aust. J. Agric. Res. **57**:781–789.

Serbin, S.P., Dillaway, D.N., Kruger, E.L., and Townsend, P.A. (2012). Leaf optical properties reflect variation in photosynthetic metabolism and its sensitivity to temperature. J. Exp. Bot. **63**:489–502.

Sims, D.A., and Gamon, J.A. (2002). Relationships between leaf pigment content and spectral reflectance across a wide range of species, leaf structures and developmental stages. Remote Sens. Environ. **81**:337–354.

Spielmeyer, W., Ellis, M.H., and Chandler, P.M. (2002). Semidwarf (sd-1), "green revolution" rice, contains a defective gibberellin 20-oxidase gene. Proc. Natl. Acad. Sci. USA **99**:9043–9048.

Venables, W.N., and Ripley, B.D. (2002). Modern Applied Statistics with S (New York: Springer).

Vogelmann, J.E., Rock, B.N., and Moss, D.M. (1993). Red edge spectral measurements from sugar maple leaves. Int. J. Remote Sens. **14**:1563–1575.

von Caemmerer, S. (2000). Biochemical Models of Leaf Photosynthesis (Collingwood, Australia: CSIRO Publishing).

Wang, S.S., Chen, X., Wang, Q., Li, P.H., and Cao, X.M. (2012a). Identification of the best spectral indices to remotely trace the diurnal course of water use efficiency of *Tamarix ramosissima* in the Gurbantunggut Desert, China. Environ. Earth Sci. **65**:11–20.

Wang, W., Yao, X., Yao, X., Tian, Y., Liu, X., Ni, J., Cao, W., and Zhu, Y. (2012b). Estimating leaf nitrogen concentration with three-band vegetation indices in rice and wheat. Field Crops Res. **129**:90–98.

Xu, H., Zhu, S., Ying, Y., and Jiang, H. (2006). Application of multispectral reflectance for early detection of tomato disease. Proc. SPIE, 6381. http://dx.doi.org/10.1117/12.685531.

Yao, X., Zhu, Y., Tian, Y.C., Feng, W., and Cao, W.X. (2010). Exploring hyperspectral bands and estimation indices for leaf nitrogen accumulation in wheat. Int. J. Appl. Earth Obs. **12**:89–100.

Yendrek, C.R., Tomaz, T., Montes, C.M., Cao, Y., Morse, A.M., Brown, P.J., McIntyre, L.M., Leakey, A.D., and Ainsworth, E.A. (2017). High-throughput phenotyping of maize leaf physiological and biochemical traits using hyperspectral reflectance. Plant Physiol. **173**:614–626.

Zhai, Y.F., Cui, L.J., Zhou, X., Gao, Y., Fei, T., and Gao, W.X. (2013). Estimation of nitrogen, phosphorus, and potassium contents in the leaves of different plants using laboratory-based visible and near-infrared reflectance spectroscopy: comparison of partial least-square regression and support vector machine regression methods. Int. J. Remote Sens. **34**:2502–2518.

Zhao, D.L., Reddy, K.R., Kakani, V.G., and Reddy, V.R. (2005). Nitrogen deficiency effects on plant growth, leaf photosynthesis, and hyperspectral reflectance properties of sorghum. Eur. J. Agron. **22**:391–403.

Zhu, X.G., Long, S.P., and Ort, D.R. (2008). What is the maximum efficiency with which photosynthesis can convert solar energy into biomass? Curr. Opin. Biotechnol. **19**:153–159.

Zhu, X.G., Long, S.P., and Ort, D.R. (2010). Improving photosynthetic efficiency for greater yield. Annu. Rev. Plant Biol. **61**:235–261.